Improving the match between the microwave source and the microwave transmission system at the Risø 10MeV electron linear accelerator

Fenger, J.; Hansen, J.

Publication date:
1972

Document Version
Publisher's PDF, also known as Version of record

Risö-M-1518

Risö-M-1518

Danish Atomic Energy Commission

Research Establishment Risö

ACCELERATOR DEPARTMENT

Improving the Match between the Microwave Source and the Microwave Transmission System at the Risø 10 MeV Electron Linear Accelerator

by

Jørgen Fenger and Johnny Hansen

July 1972

A. E. K. Risø

Risø - M - 1518

Risø - M - 1518

Title and author(s)

IMPROVING THE MATCH BETWEEN THE MICROWAVE SOURCE AND THE MICROWAVE TRANSMISSION SYSTEM AT THE RISØ 10 MeV ELECTRON LINEAR ACCELERATOR

by

Jørgen Fenger and Johnny Hansen

Date July 1972

Department or group

Accelerator

Group's own registration number(s)

16 pages + tables + 14 illustrations

Abstract

To achieve tolerable load conditions for the high-power microwave source at the 10 MeV linear accelerator, comprehensive measurements of various parameters in the accelerator tubes and the waveguide system were carried out. Based on the measurements a modification of the parameter-defining linac components has improved the present performance and caused a higher overall efficiency.

Copies to

Abstract to

Available on request from the Library of the Danish Atomic Energy Commission (Atomenergikommissionens Bibliotek), Risø, DK-4000 Roskilde, Denmark.
Telephone: (03) 35 51 01, ext. 334, telex: 43116

Fi 25-204

ISBN 87 550 0148 3

CONTENTS

I. INTRODUCTION

Owing to irregularities in the high-power microwave system of the accelerator, whereby two klystrons were damaged, measurements were carried out in order to investigate in detail the working parameters of the system. Based on the measurements a modification of the system was worked out for re-establishing acceptable performance by the klystron. The margin of safe operation was decreased, demanding protection and improvement of the components defining the working parameters.

II. DESCRIPTION

1. The Linear Accelerator Principle

The accelerator is a linear, pulsed, disc-loaded type with two accelerator tubes each of which is fed from a common, high-power microwave klystron. Fig. 1 shows the main components of the accelerator.

The electrons emitted from the cathode are axially injected into the accelerator tubes by a high-voltage pulse of 13o kV. The injected electrons are accelerated by the microwave field (TM_{o1}) which has the electrical field vector in the longitudinal direction. Each accelerator tube consists of almost 4o concentric cavities, the axial length of which determines the phase velocity of the microwave and thus the velocity of the electrons.

The microwave from the klystron (S-band, 5 MW peak/1o kW average) is via the waveguide (TE_{1o}) and power divider fed to the accelerator tubes. By means of the phase shifter the microwave to No. 2 tube is adjusted to be in phase with the electron bunches coming from tube No. 1. The residual microwave power from the accelerator tubes is dissipated in the high-power water loads. In the klystron and accelerator tubes a vacuum of $1o^{-6}$ mm Hg is maintained, whereas the waveguide system is pressurized to 1 ato (CF_2Cl_2, Freon). The klystron and accelerator tubes are separated from the waveguides by ceramic RF-windows.

2. Standing-Wave Measurements

The resultant load impedance of the waveguides and the accelerator tubes has to match the characteristic impedance of the klystron. In case of a mismatch, power is reflected and standing waves occur in the microwave system. Increase of the electrical field strength and heating of the microwave components and the insulating gas may lead to discharge at discontinuities. A voltage break-down in a ceramic window may cause a leakage and let the insulating gas into the vacuum system. This is what happened to the klystrons which were damaged.

The load conditions can be expressed by the voltage standing-wave ratio S, which is the ratio of the maximum and minimum intensities of the electric field in the guide

$$S = \frac{|V_{max}|}{|V_{min}|}.$$

The voltage standing-wave ratio can be measured with a slotted-line section at low power (5mW) from a modulated microwave generator. This way of measuring is rather precise when performed correctly. The set-up for measuring S is shown in fig. 2. The standing-wave ratio can also be expressed by the incident (P^+) and reflected (P^-) power:

$$S = \frac{\sqrt{P^+} + \sqrt{P^-}}{\sqrt{P^+} - \sqrt{P^-}}.$$

By using a directional coupler (directivity D≥45 dB) the standing-wave ratio for the complete system can be measured at high power (1o kW) from the klystron. The values measured in this way will normally be different from the low-power measurements with the slotted-line section, because of heating of the microwave components.

The standing-wave ratio of the load for the klystron is typically 1.1 and must not exceed 1.3.

The phase of the microwave to No. 2 accelerator tube is changed by means of a phase shifter. When the accelerator is trimmed, the phase of the reflected power will change, too. This means that the resultant, reflected power to the klystron and thus the impedance match of the klystron depend on the phase-shifter position. A relatively low standing-wave ratio of each of the accelerator tubes may then result in a too high standing-wave ratio at the klystron output.

3. Measurements of the Load Conditions of the Accelerator Tubes.

In order to achieve tolerable load conditions both accelerator tubes have to be matched to the characteristic impedance of the microwave transmission system. Comprehensive measurements on the tubes explained the load conditions, which are dependent on frequency, temperature, and pressure.

Fig. 3 shows the present and the original standing-wave ratio for No. 1 accelerator tube as a function of frequency. It is seen that the standing-wave ratio has changed, but is still acceptable at the frequencies 2854.o and 2856.5 MHz. This alteration may be caused by material deformation, creeping, in the tube structure. The same measurements on No. 2 tube (fig. 4) shows a very drastic change of the standing-wave ratio.

On comparison of the curves for both tubes it is seen that it has been possible to operate the accelerator at 2855 MHz with a reasonable standing-wave ratio. But a relatively small change of the klystron frequency at trimming of the accelerator easily result in an intolerable standing-wave ratio.

The aggravation of the load impedance of No. 2 tube could be caused by a deformation of the inner surface of the tube structure as a result of the

hitting of the electron beam. An inspection of the inside of the tube with a borescope did not show any local deformation, but the surface was covered with a thin layer of carbon getting thicker at the downstream end of the tube. The carbon layer is the result of a fire (1967) in the radiation zone whereby the debris of burned polyethylene was sucked into the accelerator tube. At that time it was attempted to remove the carbon layer by glow discharge in the tube, which did remove a great deal of carbon, but some was still left. Attempts were now made to remove the rest of the carbon, but as the tube structure is very complicated, a complete cleaning was impossible and no appreciable change in the standing-wave ratio was obtained.

The surface condition of the wall structure in the cavities of the accelerator tube determines the shunt resistance r_o and thus the characteristic impedance Z_o. The shunt resistance is given by:

$$r_o = K \frac{\lambda}{\delta} \quad [\text{ohm/metre}]$$

where K depends on the geometrical dimensions of the cavities, λ is the free-space wavelength, and δ the skin depth of the microwave into the wall structure. At 3 GHz, δ is 1.5 µm for copper and 65 µm for carbon. As the carbon layer is of the same order of magnitude as the skin depth in carbon, it will influence r_o. A change of Z_o from the characteristic impedance causes multi-reflections and standing waves in the electromagnetic field. Besides mismatching the klystron, this means reduced efficiency at the conversion of microwave power into electron-beam power and increased energy inhomogeneity of the electron beam (orbit instabilities of the electrons).

4. The Load Variation of the Accelerator Tubes with Temperature and Frequency.

As seen from the measurements, figs. 3 and 4, the accelerator tubes do not have an impedance match at the same frequency, and this leads to unacceptable load conditions of the klystron, when the phase of the reflected power from No. 2 tube is changed. Measurements demonstrated that the characteristic of the standing-wave ratio minimum for both tubes varied linearly with temperature and frequency

$$\frac{\Delta f}{\Delta T} = -0.0445 \quad [\text{MHz}/^{\circ}\text{C}].$$

By changing the temperature on one of the accelerator tubes it is possible to obtain a minimum standing-wave ratio of the tubes at the same frequency. Fig. 5 shows the upper standing-wave ratio minimum of both of the tubes as a function of temperature and frequency. The frequency was chosen to be 2856.2 MHz, which presupposes a temperature of 31.0°C and 42.5°C for tubes 1 and 2 respectively.

5. Impedance Matching of No. 2 Accelerator Tube.

Even at coincidence of the standing-wave ratio minima of both tubes the frequency band pass is very narrow. Fig. 6 shows the calculated maximum and minimum values of the standing-wave ratio as a function of frequency for the complete system.

To achieve a suitable frequency band pass a matching of No. 2 tube was necessary. The match is performed as a discontinuity described as a four-terminal lumped-constant circuit (Appendix 1).

The discontinuity can be a rod or a diaphragm placed in the waveguide cross section. The band width of this sort of impedance transformation is for a rod 5 MHz at S = 1.1, and for a diaphragm 1.5 MHz at S = 1.1. Both of them match the narrow band pass of the No. 2 tube, which is 0.2 MHz at S = 1.1 sufficiently well. A first experiment with a round rod configuration caused sparks between the rod and the waveguide wall. A window diaphragm match did not give any arc problems.

Fig. 7 shows the standing-wave ratio for both tubes after temperature regulation and matching of No. 2 tube. The calculated maximum and minimum values of the standing-wave ratio as a function of frequency for the complete system is seen from fig. 8. Fig. 9 shows the measured standing-wave ratio at low power, 5 mW, as a function of the phase-shifter position ($\Delta\varphi > 360^\circ$) at $f = 2856.2$ MHz, whereas fig. 10 shows the standing-wave ratio measured as the transmitted and reflected power at 10 kW from the klystron. From changing of the frequency it appeared that the best load condition of the klystron at full microwave power was at 2856.0 MHz with the previously found inlet cooling water temperatures of 31° and 42.5°C. At this frequency the standing-wave ratio varied from 1.05 to 1.085 in the whole phase-shifter range.

6. Optimising the Conversion Efficiency of the Accelerator.

After optimizing the load parameters of the microwave system the optimum conversion of microwave power into electron-beam power for each tube was found, i.e. the frequency giving the right phase velocity. By varying the frequency the electron-beam current at constant energy and the residual microwave power from the accelerator tubes were measured. The frequency variation, $\pm$ 0.2 MHz, performs a variation in the load impedance and consequently in the transmitted microwave power (2%) to the tubes, but the effects of the electron current and the residual power are much higher. At optimum conversion the residual microwave power from the tubes is minimum.

The measurements made it evident that No. 1 tube had maximum efficiency at 2856.1 MHz and No. 2 tube at 2856.0 MHz at the previously established cooling water temperatures. The ratio of residual power to minimum residual power as a function of frequency is shown for both of the tubes in fig. 11. Further the relative electron-beam current at constant energy is measured as a function of frequency, fig. 11b.

From these measurements and the standing-wave ratio measurements (section 5) the working frequency of the accelerator is determined to be 2856.0 MHz. The load line of the accelerator, fig. 12, shows the peak electron-beam current in relation to the energy.

7. Control Equipment

From the measurements on the microwave system it follows that the margin for safe operation of the accelerator had been decreased. On account of this the control of the system parameters was improved and extended:

The temperature regulation of the accelerator tubes was improved to $\pm$ 1°C.

The high-power voltage regulation was improved to $\pm$ 0.5%.

The stability of the microwave frequency was improved to $\pm$ 25 kHz ~ $\pm$ 0.1%.

An instrument controlling the microwave frequency was constructed, fig. 13.

A detector, detecting arcs on the ceramic window of the klystron was constructed, Appendix 2.

An instrument for continuous measurements of the standing-wave ratio was constructed, Appendix 3.

The measurement of the reflected microwave power was improved.

8. Conclusion

From the measurements the failure in the microwave system of the accelerator can be explained as insufficient impedance matching between the individual microwave components, particularly the accelerator tubes. The impedance of the components has changed with time, but expecially the contamination of No. 2 tube at the fire in 1967, has caused unacceptable load conditions for

the klystron. Coincidence of disadvantageous working conditions such as a relatively high output power from the klystron, overvoltage in the modulator, unfavourable phasing of the accelerator tubes, and a possible degradation of the insulating gas in the waveguides may have caused the destruction of the klystron.

A number of measurements on the accelerator proper were performed, leading to an improvement of the working parameters. The new set of working parameters of the accelerator have caused a higher efficiency, which first of all means that the klystron has to operate with less output power and consequently less marginally than earlier.

The condition of No. 2 accelerator tube is bad, but not necessarily reduced very much during the time after the fire.

An extension of the safety system and an improvement of the parameter-defining components have improved the present working condition of the accelerator.

III. REFERENCES

A.F. Harvey, Microwave Engineering. (Academic Press, London, 1963) 1313 pp.

The Stanford Two-Mile Accelerator. Edited by R.B. Neal. (W.A. Benjamin, Inc., New York, 1968) 1169 pp.

P.R. Howard, Proc. Inst. Elect. Eng., 104, part A, No. 14, 123 (1957) 139-42.

Handbook of Microwave Measurements. Edited by M. Wind and H. Rapaport. (Polytechnic Press, New York, 1958) Section 2.1.

N. Marcuvitz (ed.), Waveguide Handbook (M.I.T. Radiation Laboratory Series, 10) (McGraw - Hill, New York, 1951) 428 pp.

IV. APPENDIX

1. Matching of No. 2 Accelerator Tube

f_o = 2856.2 MHz

$z_{V_{min.}}$ = 7.31 cm, distance from the mismatch (flange of the RF-window) to the first voltage minimum ($V_{min.}$).

S = 1.14, measured voltage standing-wave ratio.

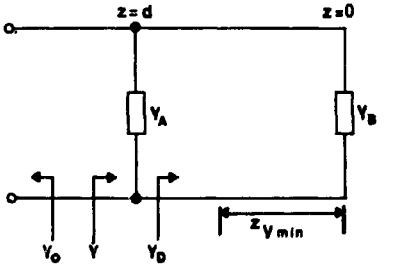

The matching in principle.

The Matching in Principle

In the figure, Y_o is the characteristic admittance of the waveguide, Y_A represents the diaphragm in the waveguide, and Y_D is the complex load admittance measured at the matching point. Paralleling of the admittances gives:

$$Y = Y_A + Y_D = (G_A + jB_A) + (G_D + jB_D). \quad (1)$$

For the waveguide: $Y_o = G_o$, Y_o real. (2)

By the impedance matching Y equals Y_o.

From (1) and (2) then follows:

$$Y = G_A + jB_A + G_D + jB_D = G_o. \quad (3)$$

A zero thickness diaphragm of an infinity conductance material will result in a pure susceptance:

$$Y_A = jB_A, \; G_A = o. \quad (4)$$

From (2), (3), and (4) it appears that:

$$G_D = G_o \quad (5)$$

$$jB_A = - jB_D. \quad (6)$$

Then the normalized load admittance in z = d:

$$\frac{Y_D}{Y_o} = Y'_D = 1 + jB'_D. \quad (7)$$

The distance z from the load to the diaphragm is chosen to obtain $G_D = G_o$, whereas $jB_A = - jB_D$ depends on the extension d' of the diaphragm into the waveguide cross section. The waveguide is considered as loss-free ($\alpha = o$).

Load impedance and reflection coefficient in a voltage minimum:

$$\left| Z_B \left(z_{V_{min.}} \right) \right| = \frac{Z_o}{S} = \frac{Z_o}{1.14} = o.878 \; Z_o \quad (8)$$

$$\left| K_B \left(z_{V_{min.}} \right) \right| = \frac{S-1}{S+1} = \frac{1.14-1}{1.14+1} = o.o654. \quad (9)$$

Load impedance and reflection coefficient at z = o (flange of RF-window):

$$\text{Arg } K_B(o) = 4\pi \frac{z}{\lambda_g} + \pi = 9.1$$

$$K_B(o) = \left| K_B(z_{V_{min.}}) \right| e^{-j2\gamma z} = o.o654 \; e^{-j9.1} \quad (10)$$

$$Z_B(o) = Z_o \frac{1 + K_B(o)}{1 - K_B(o)} = Z_o \frac{1 + o.o654 \; e^{-j9.1}}{1 - o.o654 \; e^{-j9.1}} \quad (11)$$

λ_o = 1o.5 cm free-space wavelength

λ_g = 15.4 cm waveguide wavelength

$\gamma = \beta = \frac{2\pi}{\lambda_g}$ = 41 rad/m propagation constant.

The distance z = d between the mismatch and the diaphragm is calculated by means of the reflection coefficient and load impedance at z = d:

$$K_B(d) = K_B(o) e^{-2\gamma d} = o.o654 e^{-j9.1} \cdot e^{j4\pi \frac{d}{\lambda_g}} \; [\text{d in metre}] \quad (12)$$

$$Z'_D = \frac{Z_D}{Z_o} = \frac{1 + K_B(d)}{1 - K_B(d)} = \frac{1 + o.o654 e^{-j(9.1 - 82d)}}{1 - o.o654 e^{-j(9.1 - 82d)}} \quad (13)$$

$$Y'_D = \frac{1}{Z'_D} = \frac{1 - o.o654e^{-j(9.1 - 82d)}}{1 + o.o654e^{-j(9.1 - 82d)}} \cdot \qquad (14)$$

In (7) the real part of the normalized load admittance in z = d equals 1:

$$\text{Re } Y'_D = \frac{1 - o.o654^2}{1 + o.o654^2 + o.1308 \cos(-9.1 + 82d)} = 1 \ , \qquad (15)$$

From which z = d is calculated:

$$d = \begin{cases} (5.4 \pm 1/2p\ \lambda_g) \text{ cm} & \text{towards the generator} \qquad (16a) \\ (1.5 \pm 1/2p\ \lambda_g) \text{ cm} & " \quad " \quad " \qquad (16b) \end{cases}$$

The distance d is measured from the flange of the RF-Window.

The normalized susceptance jB'_D of the diaphragm is calculated from the imaginary part of (14) and from (16a, 16b).

$$\text{Im } Y'_D = \frac{-j\ o.1308 \sin(-9.1 + 82\ d)}{1 + o.o654^2 + o.1308 \cos(-9.1 + 82d)} \qquad (17)$$

$$\text{Im } Y'_D = jB'_D = \begin{cases} -j\ o.1289 \quad (d = 5.4 \text{ cm}) \qquad (18a) \\ j\ o.1311 \quad (d = 1.5 \text{ cm}) \qquad (18b) \end{cases}$$

(18b) is chosen, as this solution involves an inductive parallel susceptance in the shape of a thin ($c \ll \lambda_g$) metal diaphragm extending transversely across the waveguide, the edges being parallel to the electric-field vector, and thus not increasing the electric field.

$$jB_A = jB_D = -j\ o.1311 \cdot Y_o \ \text{[Siemens]} \qquad (19)$$

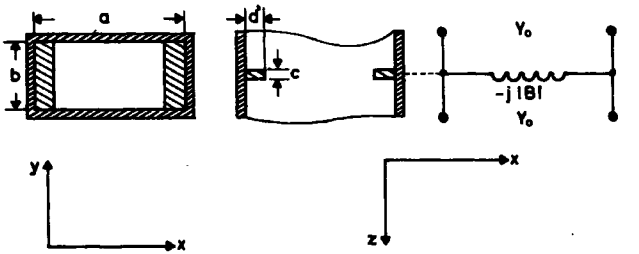

Inductive diaphragm in the rectangular waveguide.

Knowing the value of the parallel susceptance (19), the extension (d') of the diaphragm into the waveguide cross section can be calculated from the following equation ($\frac{d'}{a} \ll 1$):

$$\frac{Y_o}{B_A} = \frac{a}{\lambda_g} \cot^2 \frac{\pi d'}{a} \left(1 + \frac{2}{3} \left(\frac{\pi d'}{\lambda_o}\right)^2\right) \qquad (2o)$$

$$d'^3 + \frac{3}{2} \left(\frac{\lambda_o}{\pi}\right)^2 d' = \frac{3}{2} \frac{a\ \lambda_o^2}{\pi^3} \ \text{Arcot} \sqrt{\frac{Y_o}{B_A} \frac{\lambda_g}{a}}$$

$$d' = o.55 \text{ cm}. \qquad (21)$$

2. R.F. Arc Detector

In order to protect the klystron output window from damage caused by excessive arcing on the window surface, a photodetector is placed in the wall of an E-plane waveguide bend (Fig. 13). If an arc occurs, the detector signal will remove the microwave driver signal from the klystron within one interpulse period. The light pass to the photodetector through the wave-

guide wall is placed symmetrically on the broad side of the rectangular waveguide cutting no current paths of the TE_{10} wave. The tube for the light pass acts as a cut-off for the microwave.

3. Voltage Standing-Wave Ratio Meter

The voltage standing-wave ratio of the complete microwave system is obtained by measuring the incident and the reflected wave amplitude coupled from the waveguide by means of directional couplers placed close to the klystron.

The instrument (Fig. 14) for measuring the voltage standing-wave ratio consists of two peak-detector amplifiers, two unity gain holding circuits, and a divider module in which the ratio between the signals is derived. Multivibrator modules gate the peak-detectors and the holding circuits synchronously to the pulsing frequency of the accelerator, the lowest frequency of which is 1 pulse per second. The output from the instrument shows the standing-wave ratio in the range from 1.05 to 1.3 on a meter. Another output is connected to the fault panel of the accelerator, and in case of an excessive standing-wave ratio the microwave driver signal to the klystron is removed within one interpulse period.

The detected microwave pulses to the instrument are about 200 mV and the maximum pulse width is 7 μs. In order to follow variations during the pulse, the rise time of the peak-detector is approximately 1 μs.

The peak-detector consists of an operational amplifier and a diode-capacitor peak-detector. Negative feed-back compensates for the forward voltage drop in the diode. The amplification is adjusted to give a 10 volt output at the highest permissible standing-wave ratio, S = 1.3. A capacitor charges to the amplitude of the amplified pulse and holds the voltage. To

remove the charge of this capacitor before the next reading, the FET $Q_{1(2)}$ is conductive for a few microseconds before the next pulse. Ten microseconds after the pulse, the FET $Q_{3(4)}$ opens, and a capacitor in the holding circuit is charged to the voltage of the peak-detector output. After 50 microseconds $Q_{3(4)}$ closes, and the capacitor holds the voltage for a time determined by a discharge time constant of 100 seconds.

The ratio between the two signals from the output of the holding circuits is derived in the divider module whose output is fed to a meter, the scale of which is calibrated in voltage standing-wave ratio.

The accuracy in measuring the standing-wave ratio is not limited by the instrument proper, but by the linearity of the two microwave detector diodes. With an HP Model 420A crystal detector and an IN26 modified crystal, an accuracy of 6% is obtained in the P - 1/2P microwave power range.

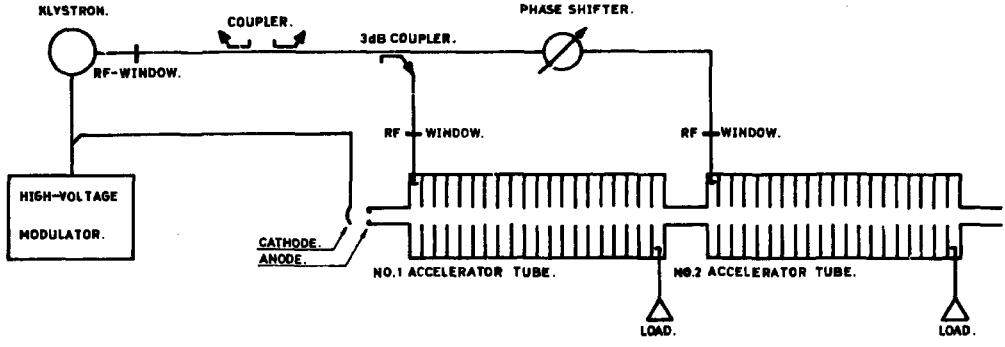

FIG.1 BLOCK DIAGRAM OF THE ACCELERATOR.

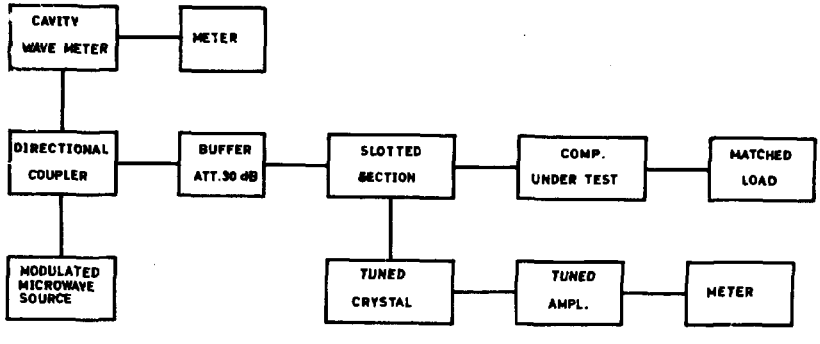

FIG.2 STANDING WAVE TEST SET.

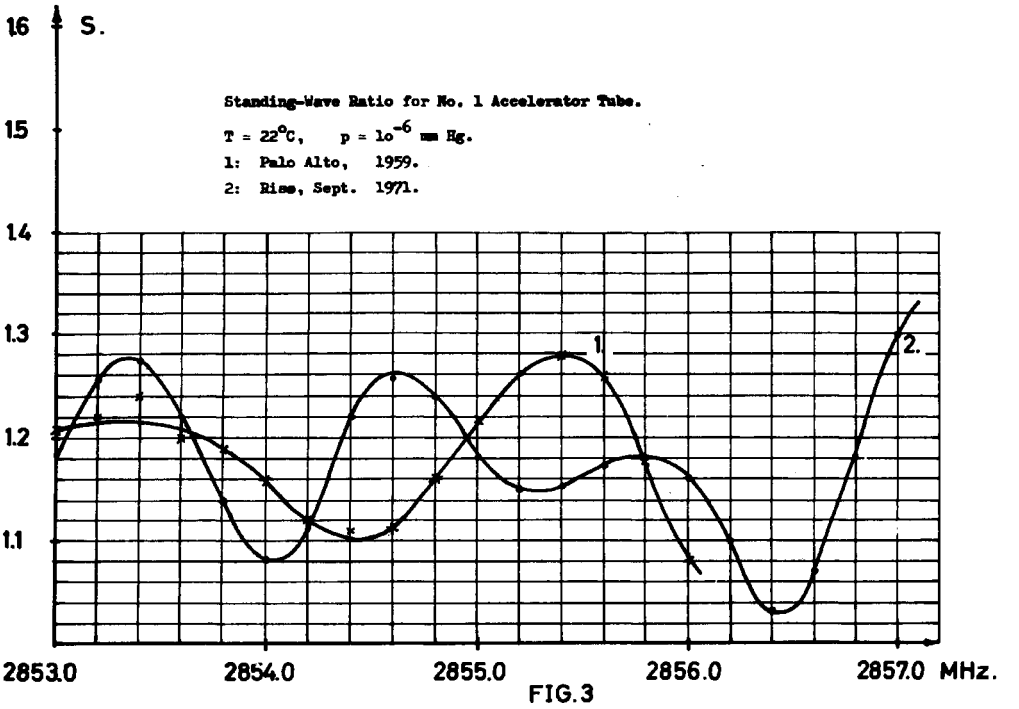
S.
1.6
1.5
1.4
1.3
1.2
1.1
Standing-Wave Ratio for No. 1 Accelerator Tube.
T = 22°C, p = 10⁻⁶ mm Hg.
1: Palo Alto, 1959.
2: Risø, Sept. 1971.
1.
2.
2853.0
2854.0
2855.0
2856.0
2857.0 MHz.

FIG.3

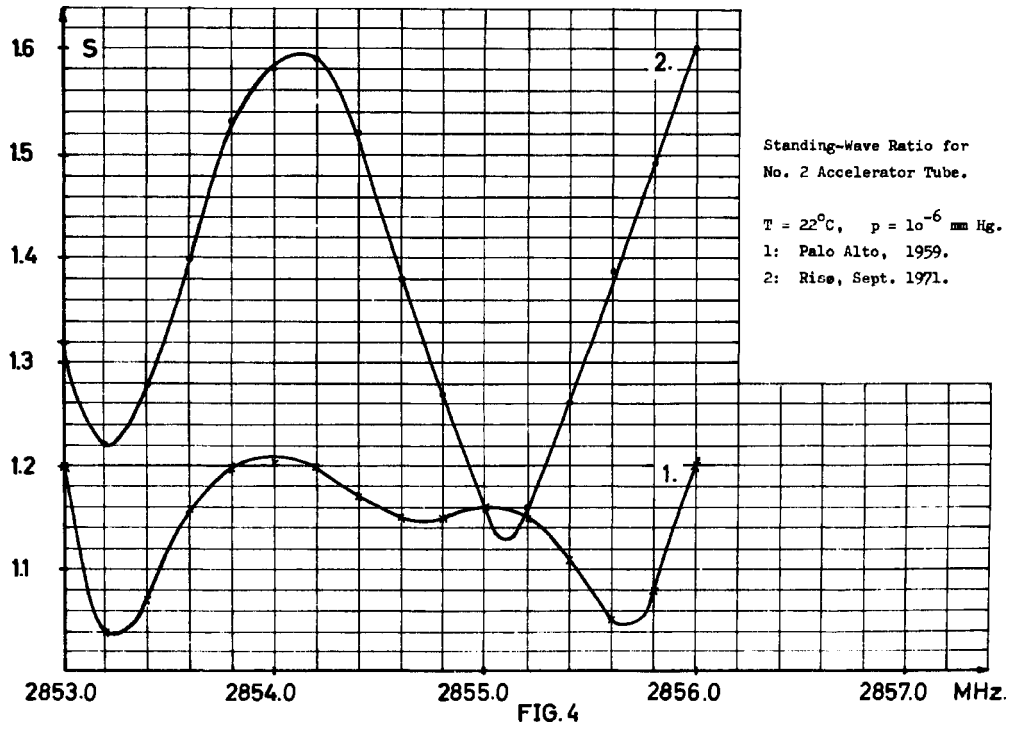
S
1.6
1.5
1.4
1.3
1.2
1.1
2.
1.
Standing-Wave Ratio for
No. 2 Accelerator Tube.
T = 22°C, p = 10⁻⁶ mm Hg.
1: Palo Alto, 1959.
2: Risø, Sept. 1971.
2853.0
2854.0
2855.0
2856.0
2857.0 MHz.

FIG.4

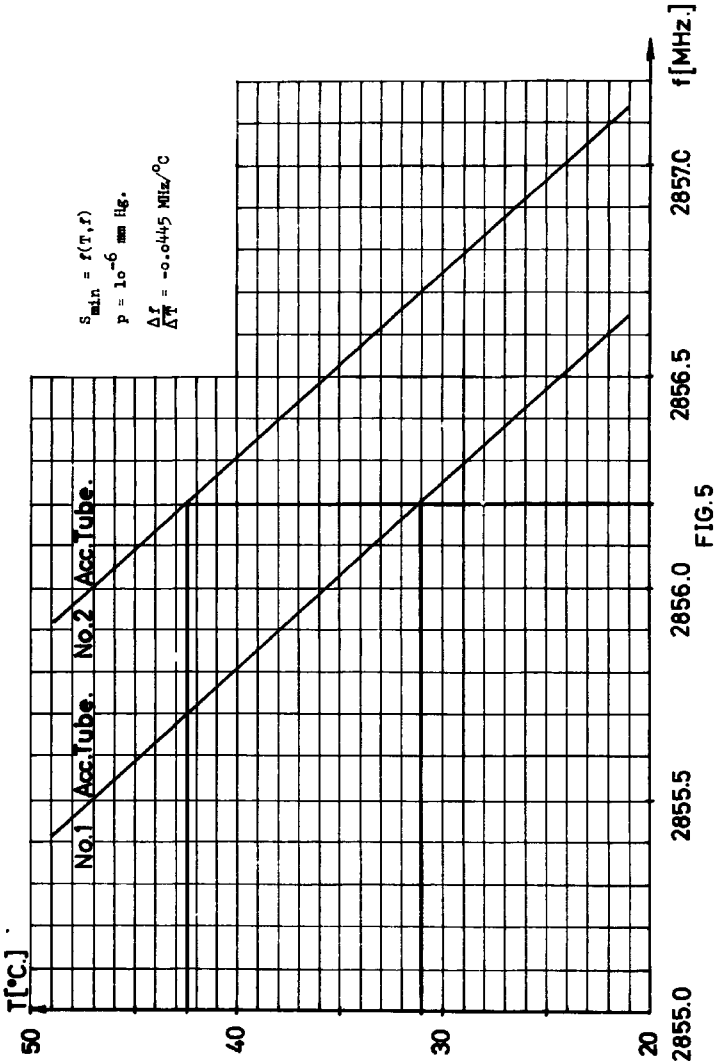

FIG.5

Calculated Maximum and Minimum
Values of the Standing-Wave Ratio.

No. 1 Acc. Tube T = 31°C
No. 2 Acc. Tube T = 42.5°C
$p = 10^{-6}$ mm Hg.

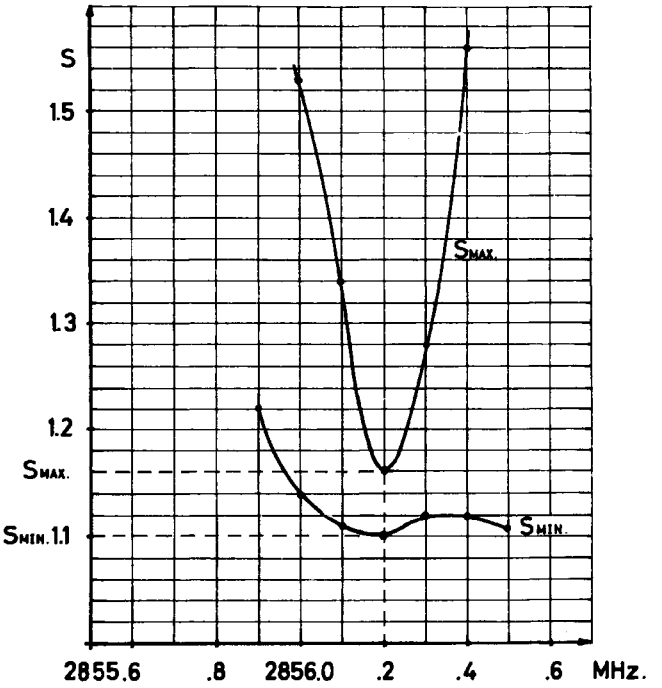

$S_{MAX} = S_{No.\ 1\ Acc.} \cdot S_{No.\ 2\ Acc.}$ $S_{MIN} = \frac{S_{No.\ 2\ Acc.}}{S_{No.\ 1\ Acc.}}$

FIG.6

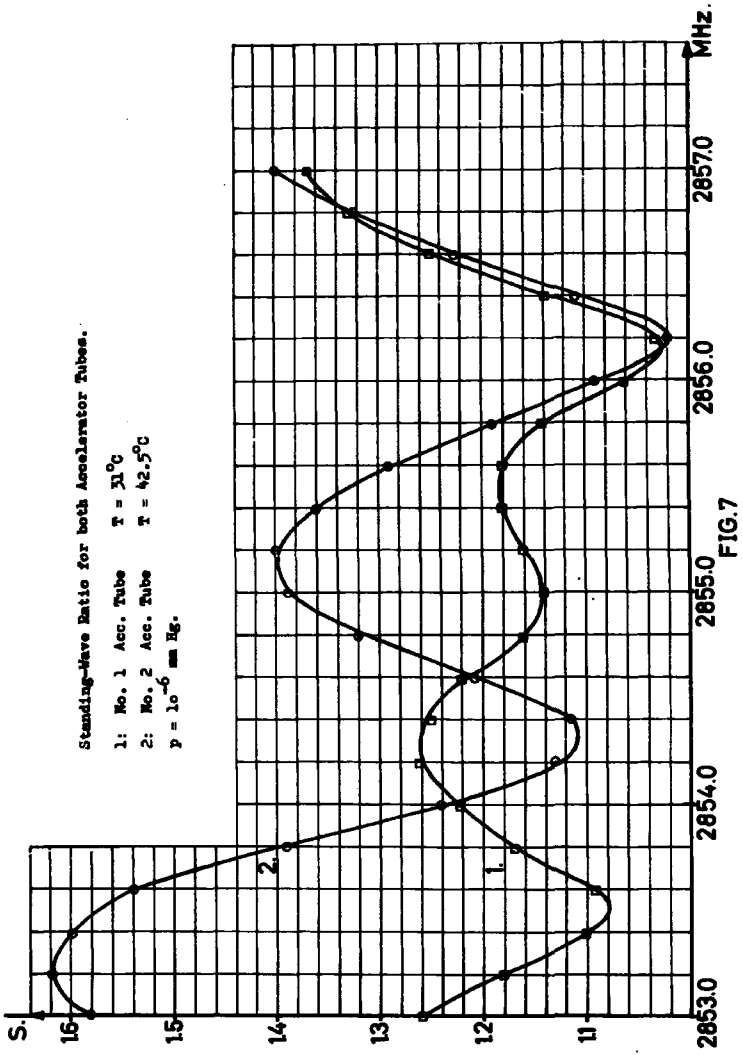

FIG.7

Calculated Maximum and Minimum Values of the Standing-Wave Ratio.

No. 1 Acc. Tube T = 31°C

No. 2 Acc. Tube T = 42.5°C

$p = 10^{-6}$ mm Hg.

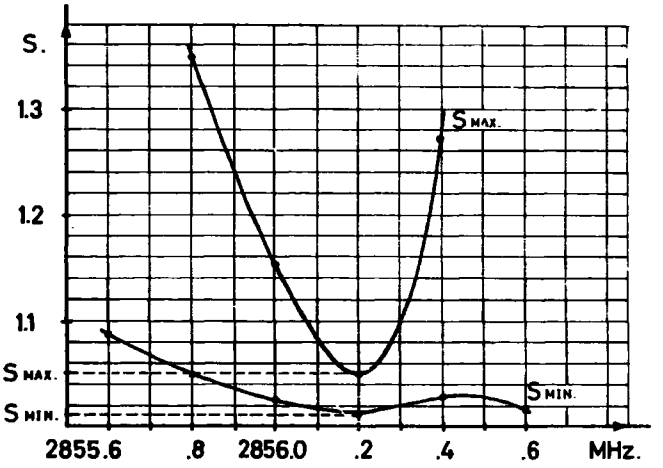

$S_{MAX} = S_{No.\ 1\ Acc.} \cdot S_{No.\ 2\ Acc.}$ $\qquad S_{MIN} = \frac{S_{No.\ 2\ Acc.}}{S_{No.\ 1\ Acc.}}$

FIG.8

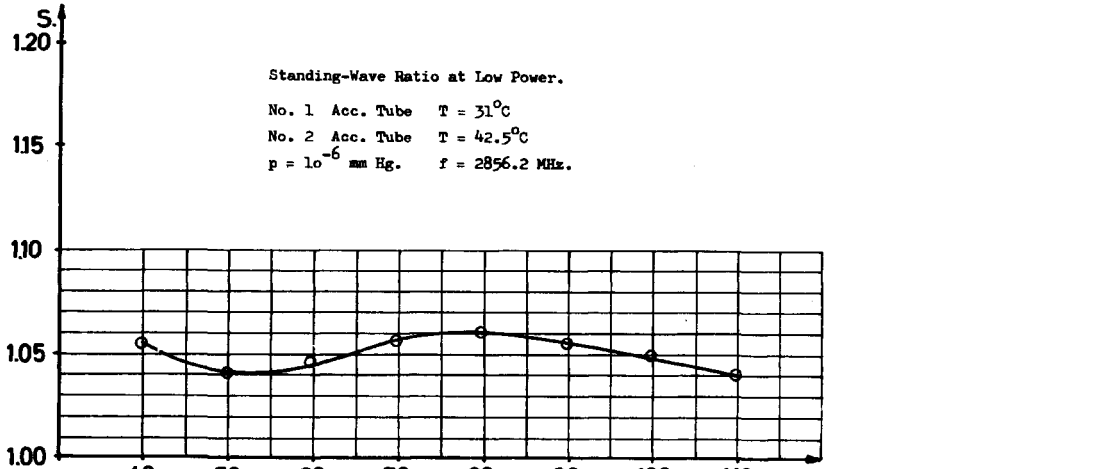
S.
1.20
1.15
1.10
1.05
1.00
Standing-Wave Ratio at Low Power.
No. 1 Acc. Tube T = 31°C
No. 2 Acc. Tube T = 42.5°C
p = 1o-6 mm Hg. f = 2856.2 MHz.
40
50
60
70
80
90
100
110 Phase shifter pos., relative

FIG.9

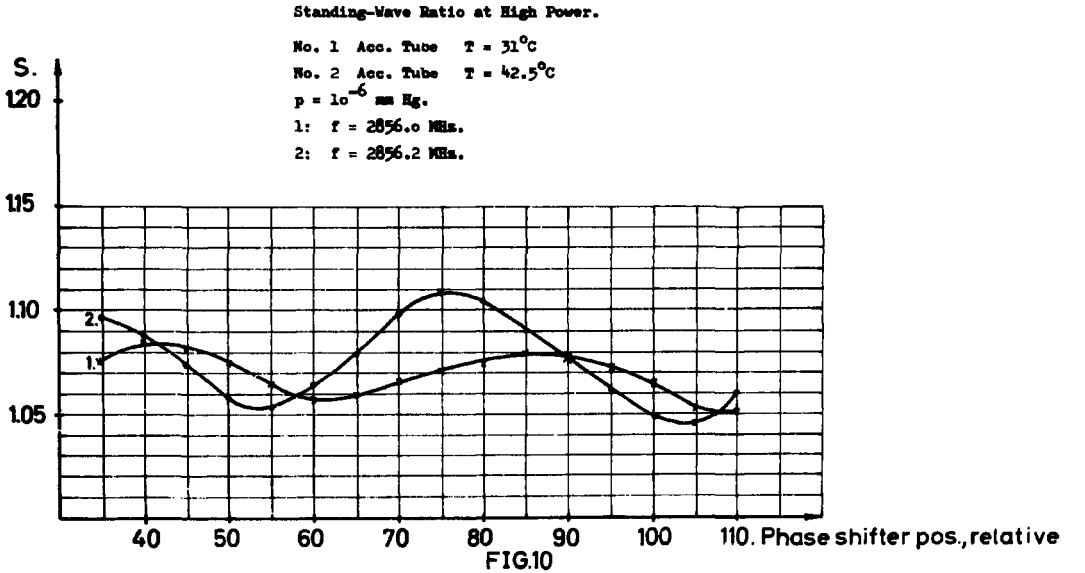
Standing-Wave Ratio at High Power.
No. 1 Acc. Tube T = 31°C
No. 2 Acc. Tube T = 42.5°C
p = 1o-6 mm Hg.
1: f = 2856.0 MHz.
2: f = 2856.2 MHz.
S.
120
115
110
105
2.
1.
40
50
60
70
80
90
100
110. Phase shifter pos., relative

FIG.10

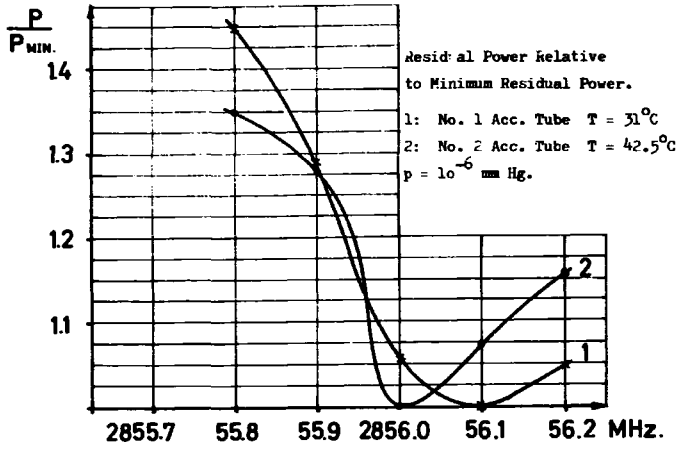

FIG. 11a

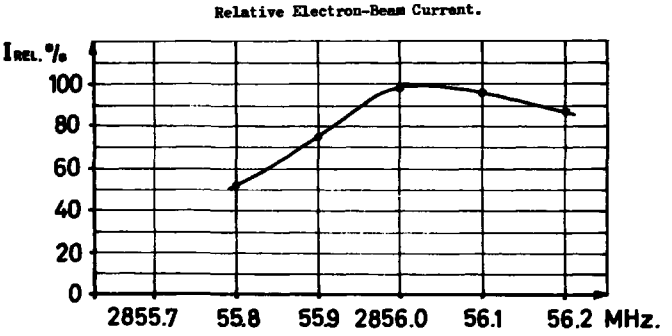

FIG.11b

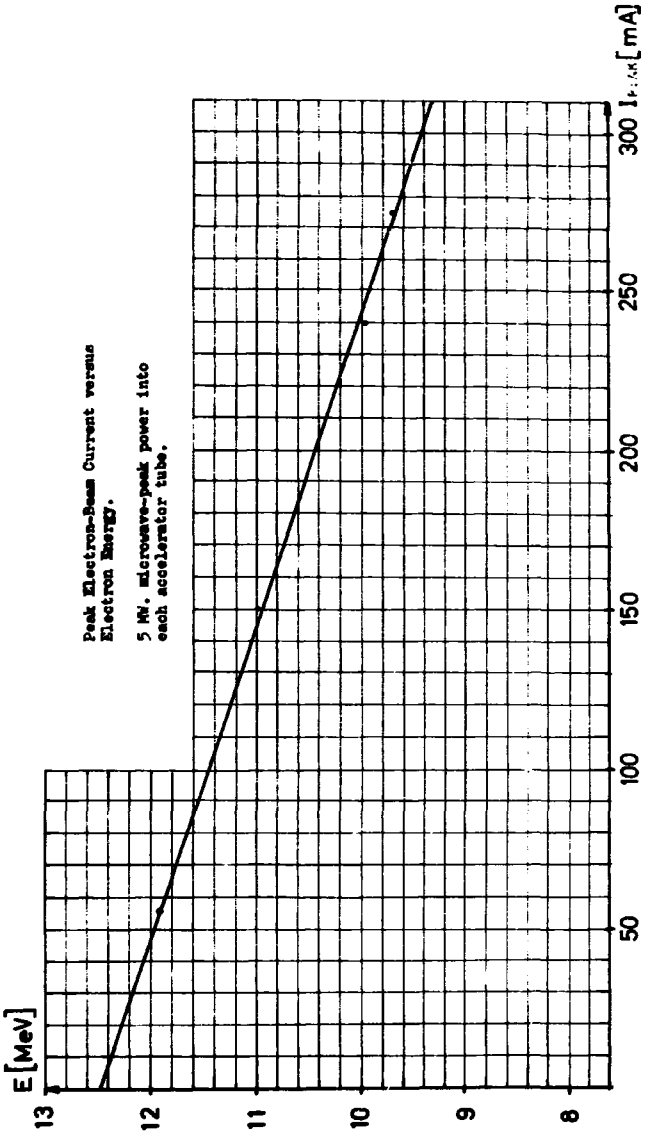

FIG.12. ACCELERATOR LOAD LINE.

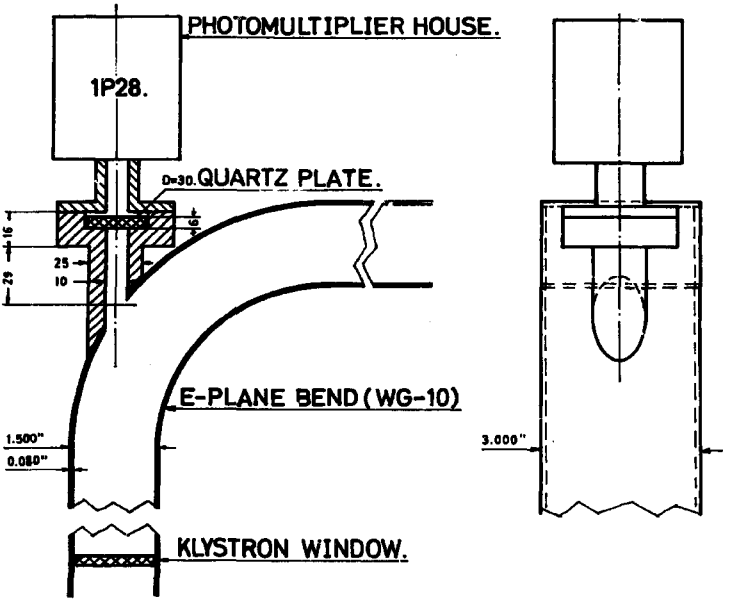

FIG.13 LIGHT PASS THROUGH THE WAVEGUIDE WALL.

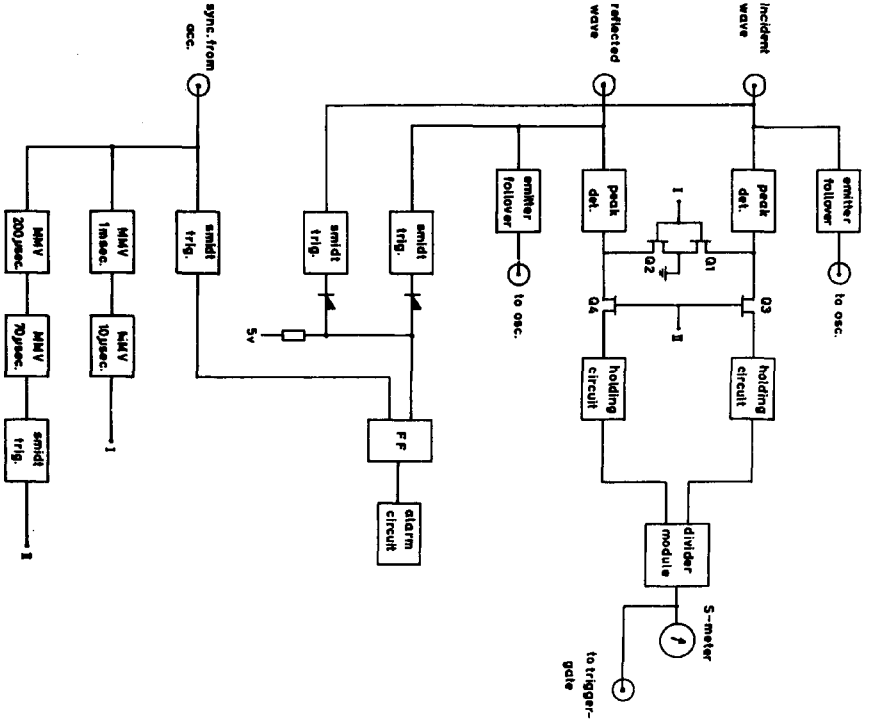

Voltage Standing-Wave Ratio Meter

FIG.14